Published in final edited form as:
J Neurophysiol. 2008 January ; 99(1): 49–59. doi:10.1152/jn.00211.2007.

Cyclophosphamide-Induced Bladder Inflammation Sensitizes and Enhances P2X Receptor Function in Rat Bladder Sensory Neurons

Khoa Dang[1], **Kenneth Lamb**[1], **Michael Cohen**[2], **Klaus Bielefeldt**[3], and **G. F. Gebhart**[1]

1*Department of Pharmacology, Carver College of Medicine, The University of Iowa, Iowa City, Iowa*

2*Department of Pathology, Carver College of Medicine, The University of Iowa, Iowa City, Iowa*

3*Internal Medicine, Carver College of Medicine, The University of Iowa, Iowa City, Iowa*

Abstract

We studied sensitization of retrogradely labeled bladder sensory neurons and plasticity of P2X receptor function in a model of cystitis using patch-clamp techniques. Saline (control) or cyclophosphamide (CYP) was given intraperitoneally to rats on days 0, 2, and 4. On day 5, lumbosacral (LS, L6–S2) or thoracolumbar (TL, T12–L2) dorsal root ganglia were removed and dissociated. Bladders from CYP-treated rats showed partial loss of the urothelium and greater myeloperoxidase activity compared with controls. Bladder neurons from CYP-treated rats were increased in size (based on whole cell capacitance) compared with controls and exhibited lower activation threshold, increased action potential width, and greater number of action potentials in response to current injection or application of purinergic agonists. Most control LS bladder neurons (>85%) responded to ATP or α,β-metATP with a slowly desensitizing current; these agonists affected only half of TL neurons, producing predominantly fast/mixed desensitizing currents. CYP treatment increased the fraction of TL bladder neurons sensitive to purinergic agonists (>80%) and significantly increased current density in both LS and TL bladder neurons compared with control. Importantly, LS and TL neurons from CYP-treated rats showed a selective increase in the functional expression of heteromeric $P2X_{2/3}$ and homomeric $P2X_3$ receptors, respectively. Although desensitizing kinetics were slower in LS neurons from CYP-treated compared with control rats, recovery kinetics were similar. The present results demonstrate that bladder inflammation sensitizes and increases P2X receptor expression and/or function for both pelvic and lumbar splanchnic pathways, which contribute, in part, to the hypersensitivity associated with cystitis.

INTRODUCTION

About 16% of adult men and women report problems with micturition (Tubaro 2004), including increased urinary frequency, urgency, and urinary incontinence. Although multiple disorders may contribute to these symptoms, interstitial cystitis (IC)/painful bladder syndrome is especially troublesome because affected individuals report significant discomfort and pain in addition to urinary symptoms (Burkman 2004; Nickel 2004). Pain is the most troubling symptom to IC patients (Parsons 2002) and 94% of registrants in an IC database report pain referred to the pelvic area (Kirkemo et al. 1997). No infectious agent causing IC has been

Address for reprint requests and other correspondence: G. F. Gebhart, Director, Center for Pain Research, University of Pittsburgh, W1444 BST, 200 Lothrop St., Pittsburgh, PA 15213 (E-mail: gebhartgf@upmc.edu)..
Present addresses: K. Bielefeldt, Department of Medicine, Division of Gastroenterology, Hepatology, and Nutrition, University of Pittsburgh, 3550 Terrace Street, Pittsburgh, PA 15261; G. Gebhart, Departments of Anesthesiology, Neurobiology, and Pharmacology, University of Pittsburgh, 3550 Terrace Street, Pittsburgh, PA 15261.

identified, although bladders of many IC patients show signs of inflammation, including edema, vasodilatation, and infiltration of mast cells (Burkman 2004; Nickel 2004).

Changes in sensory input from the bladder (i.e., bladder hypersensitivity) play an important role in the development of IC (Ness et al. 2005). IC is associated with an increased release of adenosine triphosphate (ATP) from bladder urothelial cells (Sun et al. 2001) and ATP is also released from bladder urothelium in response to stretch or bladder distension (Ferguson et al. 1997; Vlaskovska et al. 2001). Importantly, interactions between the urothelium and bladder nerve terminals are thought to regulate micturition and nociception (Andersson 2002; Kirkemo et al. 1997; Meen et al. 2001; Ness et al. 2005; Tubaro 2004; Vlaskovska et al. 2001), and ATP and P2X receptors have been implicated in bladder nociception (Ford et al. 2006; Rapp et al. 2005). For example, both $P2X_2$ and $P2X_3$ receptor knockout mice exhibit bladder hyporeflexia (Cockayne et al. 2000, 2005) and recordings from bladder primary afferent fibers show attenuated responses to mechanical bladder stimulation (Vlaskovska et al. 2001). $P2X_2$ and $P2X_3$ receptor expression is increased in the urothelium of IC patients (Tempest et al. 2004).

The bladder is innervated by pelvic and lumbar splanchnic nerves with cell bodies, respectively, in lumbosacral (LS, L6–S2) and thoracolumbar (TL, T13–L2) dorsal root ganglia (DRGs). Most studies have focused on the role of the pelvic nerve, transection of which abolishes bladder contractions in response to repetitive filling, suggesting that the pelvic nerve is important for the sensation of bladder distension and micturition (Kontani and Hayashi 1997; Meen et al. 2001). However, the lumbar splanchnic nerve is also activated by mechanical and chemical stimulation of the bladder and may play an important role in regulation of micturition and painful sensations after bladder irritation/damage (Mitsui et al. 2001; Moss et al. 1997). In addition, recent evidence suggests that different nerves innervating a visceral organ mediate different functions (Brierley et al. 2004; Dang et al. 2005a; Lamb et al. 2003). Consistent with this notion, bladder lumbar splanchnic afferents have been reported to respond more vigorously to chemical stimuli than do pelvic nerve counterparts (Moss et al. 1997).

In the present report, we used a well-established model of urinary bladder inflammation (Bon et al. 1997, 2003; Lanteri-Minet et al. 1995) to examine the consequences of inflammation on characteristics of TL and LS bladder neurons in the rat, focusing on their sensitivity to purinergic receptor agonists. We hypothesized that changes in the excitability and sensitivity of bladder sensory neurons to endogenous purinergic receptor agonists contribute to bladder dysfunction, discomfort, and pain that characterize bladder disorders such as cystitis. Portions of these data have appeared in a preliminary form (Dang et al. 2005c).

METHODS

Male Sprague–Dawley rats (200–300 g; Harlan, Indianapolis, IN) were used throughout. Rats were housed under a 12-h light and dark cycle with free access to food and water. Animal handling adhered to the *Guide for the Care and Use of Laboratory Animals* (National Research Council); the experimental protocol was approved by the Animal Care and Use Committee, The University of Iowa.

Bladder inflammation, histology, and myeloperoxidase (MPO) activity

Systemic administration of cyclophosphamide (CYP), which is metabolized to the bladder irritant acrolein (Cox 1979), causes hemorrhagic cystitis in humans and produces a cystitis-like condition in rodents (Bon et al. 1997,2003;Lanteri-Minet et al. 1995). Saline (control) or CYP (100 mg/kg) was administered systemically [intraperitoneally (ip)] on days 0, 2, and 4. On day 5, four rats from each group were killed (see following text) and the bladders removed, fixed in paraformaldehyde (4%), paraffin-mounted, and cut at a thickness of 10 μm. Sections were stained with hematoxylin and eosin (both at 5%), mounted, and examined microscopically

at both ×100 and ×400 magnifications by a pathologist. To further quantify bladder inflammation, we measured MPO activity in bladder tissue from an additional six rats/group. Rats were anesthetized, the bladders removed rapidly, minced, homogenized in ice-cold 50 mM phosphate buffer (pH 6) containing 0.5% hexadecyltrimethyl-ammonium bromide, centrifuged at 1,000 rpm for 5 min, and the supernatant was retained. In the presence of hydrogen peroxide (30%) and *o*-dianisidine dihydrochloride (0.5%), the absorbance of the supernatant was determined with a U2001 photometric reader (Hitachi, Naperville, IL).

Bladder neuron labeling and bladder inflammation

Under pentobarbital anesthesia (50 mg/kg, ip), the bladder was surgically exposed (lower abdominal incision ~1 cm in length) and 1,1′-dioctadecyl-3,3,3,′3′-tetramethylindocarbocyanine perchlorate [$DiI_{(18)}$; 100 mg in 2 ml DMSO; Molecular Probes, Eugene, OR] was injected into six to eight sites within the wall of the bladder base around the trigone using a 30-gauge needle (6 μl per site). Any visible leakage of DiI from the injection site was removed with a cotton swab. Surgery was short in duration (typically <60 min) and the depth of surgery was assessed by toe pinch extensor withdrawal. The incision was closed with 4.0 silk suture and rats were allowed to recover. Postoperative analgesia was provided by buprenorphine (2 mg/kg, ip). In four rats, Fast Blue (FB; 5% in saline; EMS-Chemie, Gross Umstadt, Germany) was injected as described earlier for DiI. Two to 3 wk later, saline (control) or CYP (100 mg/kg) was administered systemically (ip) on days 0, 2, and 4. On day 5, rats were deeply anesthetized (pentobarbital 150 mg/kg, ip) and lumbosacral (LS, L6–S2) or thoracolumbar (TL, T13–L2) DRG were harvested for acute dissociation and whole cell recordings. After removing DRG, we opened the abdomen, examined the pelvic area for leakage of dye, noted the macroscopic appearance of the bladder, removed the bladder, and measured its wet weight after emptying the contents. Euthanasia was accomplished by exsanguination after removal of the bladder.

To confirm the specificity of retrograde labeling for bladder neurons, we injected DiI into the bladder wall of four rats as described earlier. At the same time, we injected fast blue (FB) into the parietal peritoneum adjacent to the bladder. Two to 3 wk later, TL DRGs (T13–L2) were removed, fixed in 4% paraformaldehyde, cryoprotected, cut at a thickness of 10 μm, and examined by fluorescence microscopy (see following text). We studied only TL DRGs because the cell bodies of neurons that innervate the parietal peritoneum (and bladder) are located in thoracolumbar DRGs (Applebaum et al. 1980; Tanaka et al. 2002).

Cell dissociation and plating

The general protocols for harvesting DRGs and acute cell dissociation have been previously described (Dang et al. 2004, 2005a,b). Briefly, after removal, ganglia were minced and incubated at 37°C, 5% CO_2 for 60 min in serum-free, supplemented Neuro-A medium (B27 supplements: 5%; L-glutamine: 0.5 mM; penicillin/streptomycin mixture: 1%; all from Gibco, Invitrogen, Grand Island, NY) containing collagenase (type 4; 2 mg/ml), and trypsin (1 mg/ml; from Worthington Biochemical, Lakewood, NJ). Tissue fragments were gently triturated to encourage cell dissociation. Cells were collected by 5-min centrifugation at 150 *g* and washed three times with supplemented Neuro-A medium (without enzymes) and resuspended in supplemented, enzyme-free Neuro-A medium. The cells were plated on poly-D-lysine–coated coverslips (Becton Dickinson Labware, Bedford, MA) and incubated at 37°C, 5% CO_2 for 2–3 h before electrophysiological studies. Acutely dissociated neurons were round and devoid of any processes, thus reducing potential space-clamp errors. Only bladder sensory neurons (i.e., DiI- or FB-containing DRG neurons) were studied. All recordings were performed within 10 h after plating.

Solutions and electrophysiological recordings

Coverslips with cells were transferred to a recording chamber (1 ml) superfused continuously (2 ml/min) with external solution containing (in mM): NaCl 140, KCl 5, $MgCl_2$ 2, $CaCl_2$ 2, HEPES 10, and glucose 10. The pH was adjusted to 7.4 with NaOH (310 mOsm). Under low magnification (×50), neurons that innervate the bladder were identified by DiI content using a rhodamine filter and clearly showed a bright orange/red color under UV light (excitation wavelength: 530–560 nm and barrier filter: 573–648 nm). In general, <5 s were required to identify a bladder neuron. FB-labeled bladder neurons were identified using a UV-2A filter (Nikon, Tokyo, Japan; excitation wavelength: 330–380 nm and barrier filtered: 420 nm) as described earlier. Fire-polished micropipettes with tip resistances of 1.5–2 MΩ were used for current- and voltage-clamp recordings. The uncompensated series resistance was generally ≲7 MΩ. The pipette was filled with an internal solution consisting of (in mM): KCl 130, $CaCl_2$ 1, $MgCl_2$ 1, EGTA 10, HEPES 10, Na_2ATP 4, Tris-GTP 0.5, and GDP 0.5. The pH was adjusted to 7.2 using KOH (310 mOsm). After establishing the whole cell configuration, the voltage was clamped at −70 mV using an Axopatch 200B amplifier (Axon Instruments, Union City, CA), digitized at 1 kHz (Digidata 1350, Axon Instruments), and controlled by Clampex software (pClamp 9, Axon Instruments). Cell capacitance was obtained by reading the value from the Axopatch 200B amplifier. Recordings began 2–3 min after establishing whole cell configuration to ensure stable recording conditions.

In current-clamp mode, resting membrane potential was determined by obtaining the value from the amplifier (Axopatch 200B). Only cells that had a resting membrane potential more negative than −40 mV and generated action potentials with a distinct overshoot >0 mV in response to depolarizing current injections were studied. action potential (AP) duration was determined at 50% of the peak amplitude from baseline. We investigated spontaneous activity by recording the baseline activity for 1 min before electrical or chemical stimulation. To identify AP threshold, a series of 10-ms current pulses in 20-pA increments (1 s apart) was injected. The minimum current (pA) required to evoke an AP was determined (rheobase) and the activation threshold (mV) was taken as the greatest membrane potential in the absence of an AP (Gold and Traub 2004). To examine firing patterns in gastric sensory neurons, suprathreshold current (2 × rheobase) was injected for 500 ms and the number of APs counted.

Drugs were applied using a fast-step SF-77B superfusion system (Warner Instruments, Hamden, CT) with a three-barrel pipette placed in close proximity (100 μm) to the cell, allowing complete solution exchange within 25 ms (Dang et al. 2005a). Agonists were applied for 4 s, whereas antagonists were superfused for 30 s before the application of agonists. A washout period of 4 min was allowed between agonist applications. Unless mentioned otherwise, drugs and chemicals were obtained from Sigma–Aldrich (St. Louis, MO) and prepared fresh from stock solutions on the day of the experiment. All experiments were performed at room temperature (21–23°C). We used current increases >20 pA or voltage changes >4 mV as thresholds to identify responses to purinergic agonists because these levels exceeded baseline variability by a factor of two. To determine the kinetics of response onset, we measured the time from 10 to 90% of peak amplitude.

Immunohistochemistry

To determine the percentage of bladder neurons expressing the $P2X_3$ subunit, we performed immunohistochemistry for $P2X_3$ protein. Fluorogold (FG, 4%; Biotium, Hayward, CA) was injected into the bladder base in eight rats as described earlier for DiI. After 2–3 wk, saline (n = 4) or CYP (n = 4) was given as described earlier. Rats were killed on day 5 and DRGs were rapidly removed, fixed in 4% paraformaldehyde for 4 h, and cryoprotected in 30% sucrose for 3 days. Frozen DRGs were sectioned at 10 μm using a Leica 3M 3050 cryostat; one section was selected every 50 μm to minimize double counting. DRG sections were blocked with 3%

goat serum in 0.01 M phosphate-buffered saline (PBS, Sigma–Aldrich) for 2 h before incubation in primary antibody (rabbit anti-rat, 1:1,000; Alamone Labs, Jerusalem, Israel) for 24 h, 4°C, after which the primary antibody was aspirated and sections were washed three times for 15 min with 0.01 M PBS. Secondary antibodies (anti-rabbit) conjugated to either Alexa Fluor 488 or 568 (Molecular Probes) were applied for 4 h and washed three times for 15 min with 0.01 M PBS. Sections were mounted with fluorescence mount (Sigma–Aldrich) and viewed with a Nikon microscope equipped with separate fluorescence filters. Images were captured with a model 2.3.1 SPOT digital camera (Diagnostic Instruments, Sterling Heights, MI). All cells positive for FG (i.e., bladder cells) were counted and the number costained with $P2X_3$ antibody was determined. For control experiments, primary antibody was omitted or blocked with a corresponding antigenic peptide for 24 h. No labeling was observed (data not shown).

Data analyses

Data are presented as means ± SE. Analyses were performed using the software package GraphPad Prism 4 (GraphPad Software, San Diego, CA). Sigmoidal concentration–response curves were generated using the following equation: $Y = A/\{1 + \exp[-(\log EC_{50} - X)/B]\}$, where X is the logarithm of concentration; Y is the response and starts at 0 and goes to A with a sigmoidal shape; and B is the Hill slope. Desensitization kinetics were fitted with a standard exponential equation: $Y = K_0 + K_1 \times \exp(-t/\tau)$, where Y is the current amplitude at time t, K_0 is the amplitude of the sustained component, and τ is the time constant. K_0 and K_1 represent the contribution to current amplitude from the fast and slow components of the current, respectively. For dichotomous variables, a chi-square test was used. Where appropriate, results were evaluated using a one-way ANOVA or Welch's *t*-test after logarithmic transformation. Results were considered to be statistically significant when $P < 0.05$.

RESULTS

CYP produces bladder damage and inflammation

Grossly, CYP treatment caused darkening of the bladder in every rat, which was not seen after saline treatment. In addition, the weight of bladders from CYP-treated rats was significantly greater than control rats (control: 101 ± 3 g, $n = 36$; CYP: 175 ± 5 g, $n = 30$; $P < 0.001$). Histologically, the bladder wall appeared thickened in CYP-treated rats compared with controls and was associated with partial loss of the urothelium. The remaining urothelial cells in CYP-treated rats were abnormally large compared with controls. Consistent with both gross and microscopic evaluations of the bladder, CYP treatment significantly increased myeloperoxidase activity relative to controls (control: 0.11 ± 0.01, $n = 3$; CYP: 0.83 ± 0.2 unit/g, $n = 3$; $P < 0.001$).

Specificity of labeling with DiI

DiI is lipophilic and leakage or diffusion from the injection site in the bladder wall could result in labeling of sensory neurons innervating adjacent tissues, which would then be misidentified as bladder sensory neurons. To address this concern, we injected FB into the bladder wall of three rats and counted FB-labeled cells on randomly chosen coverslips containing TL or LS DRG cells. Consistent with previous reports using DiI or another tracer (Dang et al. 2005a; Wang et al. 1998), significantly more bladder sensory neurons were found in LS than in TL DRG (LS: 120/1812 = 6.8 ± 0.6%; TL: 66/3268 = 2.5 ± 0.4%; $P < 0.01$); the percentages of FB-labeled bladder neurons were not different from percentages of DiI-labeled bladder neurons (5.4 ± 0.5 and 2.0 ± 0.3%; Dang et al. 2005a). It is also possible that DiI may spread within the DRG, again resulting in nonspecific labeling. We addressed this concern by injecting DiI into the bladder wall and FB into the adjacent parietal peritoneum and looked for double-labeled DRG cells. Because cell bodies of neurons innervating the parietal peritoneum and the bladder

are found in TL DRGs (Applebaum et al. 1980; Tanaka et al. 2002), we examined only TL DRGs. Of 89 DiI and 179 FB neurons examined, only 4 cells contained both dyes, demonstrating that DiI can be used to reliably and selectively label sensory neurons for whole cell study.

Bladder inflammation increases cell size and induces hyperexcitability in bladder sensory neurons

We examined the distribution of cell size and excitability of bladder sensory neurons after bladder inflammation. Using whole cell capacitance as an index of cell size, we considered neurons as small, medium, or large if whole cell capacitance was ≤20, 20.1–60, or >60 pF, respectively. As illustrated in Fig. 1, virtually all LS bladder neurons were classified as small (34/152, 22%) or medium (117/152, 77%) in size (one cell [1%] was large), consistent with previous reports (Dang et al. 2005a;Yoshimura and de Groat 1999;Yoshimura et al. 2003). In contrast, all TL neurons were medium (70/88, 80%) or large (18/88, 20%) in size.

Because incorporation of lipophilic DiI into the plasma membrane may potentially alter whole cell capacitance, and consequently mislead interpretation of cell size, we injected hydrophilic FB into the bladder wall in three rats and measured capacitance of FB-labeled LS bladder neurons to facilitate comparison with previous studies (Yoshimura and de Groat 1999; Yoshimura et al. 2003). The mean whole cell capacitance of FB-labeled LS bladder neurons (26.9 ± 1 pF, $n = 90$) did not differ from that of DiI-labeled LS bladder neurons (27.7 ± 0.6 pF, $n = 152$; $P > 0.05$). Similarly, FB-labeled LS neurons were characterized as small (26/90, 28.9%) or medium (64/90, 71.1%) in size (Fig. 1), consistent with results using DiI in both the present study and an earlier study (Dang et al. 2005a) and previous reports using FB (Yoshimura and de Groat 1999; Yoshimura et al. 2003).

Bladder inflammation significantly shifted the size distribution of LS neurons (small: 8/132, 6%; $\chi^2 = 14.9$; $P < 0.001$; medium: 123/132, 93%; $\chi^2 = 14.2$; $P < 0.001$; large 1/132; Fig. 1). Consistent with these findings, the mean cell capacitance of LS neurons significantly increased after bladder inflammation compared with control (control, 27.7 ± 0.6 pF vs. CYP, 33.4 ± 1 pF; $P < 0.001$). Although the proportions of medium (88/115, 77%) and large (27/115, 23%) TL bladder neurons were unchanged by CYP treatment, inflammation similarly increased overall mean TL cell size compared with control (control, 45 ± 1.2 pF vs. CYP, 56 ± 2 pF; $P < 0.001$).

Bladder inflammation alters active and passive membrane properties of bladder sensory neurons

LS and TL neurons differed in some of their active and passive membrane properties. Membrane potential was more negative in LS than in TL neurons, requiring greater current injection for AP generation (Table 1). Under control conditions, no bladder neurons exhibited spontaneous activity (LS: 0/23; TL: 0/23). Bladder inflammation did not alter resting membrane potential, but significant numbers of LS (11/31, 35%; $\chi^2 = 10.3$; $P < 0.01$) and TL (13/29, 45%; $\chi^2 = 13.8$; $P < 0.001$) neurons from CYP-treated rats were spontaneously active (Fig. 2, *A* and *F*; Table 1). Spontaneously active LS and TL neurons from CYP-treated rats fired 43.8 ± 14 and 53.6 ± 13 APs in 60 s, respectively, but had resting membrane potentials that did not differ from neurons without spontaneous activity (LS: −50.1 ± 1.8 mV; TL: −45.3 ± 0.7 mV; $P > 0.05$) or corresponding control groups. However, all spontaneously active neurons exhibited apparent membrane potential oscillations (oscillation amplitude: LS: 5.9 ± 0.4 mV; TL: 4.8 ± 0.3 mV). Bladder inflammation significantly lowered the rheobase of both LS and TL neurons, shifted the AP threshold to more negative potentials, and widened the AP duration (Fig. 2, *B* and *G*; Table 1). In addition, suprathreshold current injection (rheobase ×

2) in cells from CYP-treated rats evoked significantly more APs compared with control (Table 1; Fig. 2, *C* and *H*).

Bladder inflammation enhances responses to purinergic agonists

In neurons from control rats, ATP (100 μM) depolarized all LS neurons tested (23/23), triggering APs in all but 3, whereas ATP depolarized only 13/23 TL neurons, with 6 firing APs (Fig. 2, *D* and *I*). ATP produced greater-magnitude depolarization in LS bladder neurons compared with TL counterparts (LS: 24.5 ± 1.5 mV; TL: 6.2 ± 1.2 mV) that was associated with a greater number of APs (LS: 8.9 ± 0.7; TL: 3.7 ± 1.4; $P < 0.05$) (Table 1). We also applied the selective homomeric $P2X_1$, $P2X_3$, and heteromeric $P2X_{2/3}$ receptor agonist α,β-metATP (North 2002) to the same bladder neurons that were previously challenged with ATP. α,β-metATP (100 μM) depolarized 23/23 and 12/13 ATP-sensitive LS and TL neurons, respectively (Fig. 2, *E* and *J*) and triggered APs in all bladder neurons that generated APs in response to ATP (20 LS and 6 TL neurons) (Table 1).

In bladder neurons from CYP-treated rats, ATP depolarized a similar fraction of LS neurons (30/31, 97% vs. 23/23, 100% in control). In TL neurons, however, bladder inflammation significantly increased the proportion of neurons that responded to ATP (26/29, 90% vs. 13/23, 57% in control; $\chi^2 = 7.5$, $P < 0.01$). As shown in Fig. 2, *D* and *I*, ATP caused significantly greater depolarizations, resulting in AP generation in all neurons obtained from CYP-treated animals and a higher firing rate compared with controls (Table 1). Similarly, α,β-metATP triggered greater depolarizations associated with greater numbers of APs in bladder neurons from CYP-treated rats relative to corresponding control groups (Table 1 and Fig. 2, *E* and *J*).

Bladder inflammation increases purinergic currents and slows desensitization

Consistent with findings described earlier, significantly more LS than TL neurons responded to the purinergic agonists and with different desensitization kinetics (Fig. 3 and Tables 2 and 3). A slowly desensitizing current predominated in LS neurons in response to ATP (46/53, 87%) (Fig. 3*B*). Only 3 (6%) and 4 (7%) LS neurons expressed fast (Fig. 3*A*) and mixed desensitizing currents, respectively (Fig. 3, *C* and *C*′). α,β-metATP triggered similar but significantly lower peak currents in almost all of the same cells (Tables 2 and 3).

In contrast, ATP produced predominantly mixed currents in 17/33 (52%) TL neurons (Fig. 3*F*). Ten of 33 (30%; Fig. 3*E*) and 6/33 (18%; Fig. 3*D*) TL neuronsexpressed slow and rapid desensitizing currents in response to ATP, respectively. In 6 TL neurons, ATP but not the P2X receptor subtype-selective agonist α,β-metATP triggered inward currents that slowly activated and desensitized. Similar to the effects of ATP, α,β-metATP triggered slow, rapid, and mixed desensitizing currents in 4 (15%), 6 (22%), and 17 (63%) of 27 TL neurons, but with significantly lower peak current than did ATP (Table 2). Current densities for kinetically distinct currents and corresponding current kinetics in response to purinergic agonists are summarized in Tables 2 and 3, respectively.

Although CYP treatment did not alter the proportions of LS bladder neurons that responded to purinergic agonists (Table 2), LS neurons from CYP-treated rats expressed significantly greater peak current density compared with controls (Table 2; compare Fig. 3*B* with Fig. 3*B**). As in controls, both ATP and α,β-metATP triggered only slowly desensitizing currents in all LS responders (Fig. 3*B**). However, neurons obtained from animals with cystitis showed an accelerated time to peak and slower desensitization kinetics after purinergic agonist stimulation compared with controls (Table 3).

Consistent with the current-clamp data, bladder inflammation significantly increased the fraction of TL neurons that responded to purinergic agonists and increased the peak current

density compared with controls (Tables 2 and 3). ATP triggered slow, fast, and mixed desensitizing currents in 7 (15%, Fig. 3*E**), 6 (13%; Fig. 3*D**), and 34 (72%; Fig. 3*F**) of 47 TL neurons, respectively. In three TL neurons, ATP but not *α,β*-metATP triggered current that slowly activated and desensitized. Interestingly, whereas *α,β*-metATP produced a slow desensitizing current in a similar proportion of TL neurons (4/44, 9%) after bladder inflammation, the fractions of fast (19/44, 43%; $\chi^2 = 5.4$; $P < 0.05$) and mixed (21/44, 48%; $\chi^2 = 7.2$; $P < 0.01$) desensitizing currents in response to *α,β*-metATP increased and decreased significantly, respectively, relative to controls. In contrast to LS neurons, inflammation did not alter the kinetics of P2X receptor-mediated currents in TL neurons (Table 3).

Bladder inflammation does not alter the concentration–response function of purinergic agonists

To investigate whether the increase in current density after bladder inflammation is due to a change in the potency (EC_{50}) or an increase in the maximum response to purinergic agonists, we examined the concentration-dependent effects of ATP and *α,β*-metATP for the principal currents produced in LS (slow) and TL (fast/mixed) neurons. To control for differences in current densities, we expressed current as a fraction of relative current at 300 μM (I/I_{max}). As shown in Fig. 4, *A* and *B*, ATPand *α,β*-metATP–activated currents were concentration dependent for both the slow and rapid (fast) desensitizing currents with a lower EC_{50} for ATP (slow desensitizing current: 16.8 ± 3 μM; $n = 15$; fast desensitizing current: 17.6 ± 5 μM; $n = 8$) compared with *α,β*-metATP (slow desensitizing current: 43.5 ± 3 μM; $n = 20$; fast desensitizing current: 46.3 ± 6 μM; $n = 7$; $P < 0.001$ for both currents). The EC_{50} values for slow (ATP and *α,β*-metATP, respectively: 17.1 ± 4 μM, $n = 13$; 39.2 ± 4 μM, $n = 10$) and fast (ATP and *α,β*-metATP, respectively: 14.5 ± 3 μM, $n = 9$; 38.9 ± 5 μM, $n = 11$) desensitizing currents did not differ in bladder neurons from CYP-treated rats compared with control.

To examine whether purinergic agonists increase maximum currents, we plotted current densities against ATP or *α,β*-metATP concentrations in the same cells as described earlier. Bladder inflammation significantly increased the maximum current density triggered by application of ATP or *α,β*-metATP for both kinetically distinct currents compared with control (Fig. 4, *C* and *D*).

Bladder inflammation increases peak current produced by α,β-metATP relative to ATP

To examine whether ATP activates other P2 receptors for the principal currents in LS (slow) and TL (fast/mixed) bladder neurons, we sequentially applied maximum concentrations of ATP (300 μM) or *α,β*-metATP (300 μM) to some of the same neurons. In bladder neurons from control rats, ATP produced a 58 ± 3.8% ($n = 11$; $P < 0.001$; Fig. 4*C*) greater peak current than did *α,β*-metATP for the slow desensitizing current. In contrast, ATP and *α,β*-metATP evoked similar peak currents for the fast desensitizing current (5.5 ± 1.7%; $n = 5$; $P > 0.05$; Fig. 4, *D* and *E*), demonstrating that activation of other P2 receptors is, in part, responsible for a greater slowly desensitizing current in response to ATP compared with *α,β*-metATP at a lower concentration (30 μM). In neurons from CYP-treated rats, the maximum current produced by ATP relative to *α,β*-metATP was similar for the rapid desensitizing current (3.2 ± 0.4%; $n = 4$; Fig. 4, *D* and *E*, *right traces*). However, ATP produced only a 24.1 ± 2% greater peak current ($n = 9$; comparison with ATP effects on control LS neurons, $P < 0.001$; Fig. 4*C*, *right traces*) than did *α,β*-metATP, suggesting a shift to the expression of heteromeric $P2X_{2/3}$ channels, which are activated by *α,β*-metATP.

Bladder inflammation does not alter recovery kinetics of slow or fast desensitizing currents

We next examined whether bladder inflammation alters recovery kinetics for the principal currents found in LS (slow) and TL (fast/mixed) bladder neurons. Based on kinetic studies in our previous report (Dang et al. 2005), application intervals of 3 and 1 min were chosen for

fast and slowly desensitizing currents, respectively, to allow a complete recovery of P2X-mediated currents. Using a two-stimulus protocol, we followed the initial agonist application (4 s) with a second application at increasing interstimulus intervals. The fraction of current in response to the second application of α,β-metATP was normalized to the first application and plotted against time. In bladder neurons from control rats, the slow desensitizing current showed little decay and recovered rapidly, whereas the fast desensitizing component required 3 min for complete recovery. Based on single-exponential fitting, the slow desensitizing current recovered significantly faster than did the rapid desensitizing current (time constants of 11.6 ± 0.7 s, $n = 12$, and 44.1 ± 3 s, $n = 6$, respectively; $P < 0.001$). Because fast and slow desensitizing currents were rarely seen in LS and TL bladder neurons, respectively, we did not systematically examine their recovery kinetics. In bladder neurons from CYP-treated rats, recovery kinetics for slow and fast desensitizing currents appeared similar compared with control, which was confirmed by single-exponential fitting (time constants for slow and fast currents, respectively: 13.5 ± 1.6, $n = 6$; 45.8 ± 3 s, $n = 8$; $P > 0.05$ compared with controls).

Antagonism of α,β-metATP-activated currents by selective antagonists

To establish that α,β-metATP triggers currents by activating P2X receptors, we applied trinitrophenyl-ATP (TNP-ATP), a selective homomeric $P2X_1$, $P2X_3$ and heteromeric $P2X_{2/3}$ receptor antagonist (Virginio et al. 1998) to neurons from CYP-treated rats. In the presence of TNP-ATP (100 nM), the α,β-metATP–mediated slow desensitizing current was reversibly inhibited by 75.3 ± 4% ($n = 6$) relative to control (Fig. 5*A*, *left traces*). However, 5-({[3-phenoxybenzyl][(1S)-1,2,3,4-tetrahydro-1-naphthalenyl]amino}carbonyl)-1,2,4-benzenetricarboxylic acid (A317491, 10 μM), a potent and selective homomeric $P2X_3$ and heteromeric $P2X_{2/3}$ receptor antagonist (Jarvis et al. 2002), attenuated the current by only 32.7 ± 2% in the same cells (Fig. 5*A*, *right traces*). Both TNP-ATP and A317491 completely and reversibly inhibited the fast desensitizing current in all six neurons tested (examples in Fig. 5*B*). These results suggest that activation of heteromeric $P2X_{2/3}$ and homomeric $P2X_3$ receptors trigger the slow and rapid desensitizing currents, respectively.

Bladder inflammation significantly up-regulates the fraction of $P2X_3$-immunopositive TL neurons

Because significantly more TL neurons responded to purinergic agonists with fast desensitizing kinetics after bladder inflammation, we stained cells for $P2X_3$ immunoreactivity (Fig. 6). In control neurons, 89/107 (83%) LS and 39/97 (40%) TL cells showed $P2X_3$ immunoreactivity. Bladder inflammation significantly increased the fraction of TL neurons (71/104, 68%; $\chi^2 = 16$; $P < 0.001$), but not LS counterparts (87/98, 89%), that exhibited $P2X_3$ immunoreactivity.

DISCUSSION

The present report confirms and significantly extends our previously reported findings (Dang et al. 2005a) on differences between the pelvic (cell bodies in LS DRGs) and lumbar splanchnic (cell bodies in TL DRGs) innervation of the rat urinary bladder. The present results establish that neuronal excitability in both sensory pathways is significantly increased by bladder inflammation as revealed by changes in action potential threshold and spike frequency during current injection. Additional evidence is provided by the observation that about one third of bladder neurons obtained from animals with inflamed bladders were spontaneously active, whereas control bladder sensory neurons were uniformly silent. Bladder inflammation also significantly increased the peak inward current in response to application of purinergic receptor agonists and increased the proportion of TL neurons that responded to them, which was verified immunohistochemically, and altered the kinetics of currents triggered by purinergic agonists in LS neurons. Importantly, use of selective purinergic receptor ligands revealed a significant

shift in the expression of P2X receptors toward heteromeric $P2X_{2/3}$ and homomeric $P2X_3$ for LS and TL neurons, respectively, after bladder inflammation.

Consistent with prior observations in bladder, gastric, and colon sensory neurons (Bielefeldt et al. 2002; Dang et al. 2004, 2005a; Gold and Traub 2004; Sugiura et al. 2004, 2007), most rat bladder sensory neurons are medium sized as judged by their capacitance. As previously described for gastric (Dang et al. 2004) and LS bladder neurons (Yoshimura and de Groat 1999), we noted an increase in the size of LS and TL bladder neurons harvested from animals with inflamed bladders. We did not address the mechanism for the change in cell size, but others have reported similar findings in response to inflammation of the hind paw, which could be blocked by neutralization of nerve growth factor (NGF) (Nicholas et al. 1999). Prior studies have demonstrated a significant increase in NGF during CYP-induced cystitis in rats, suggesting that an increase in NGF in the target area (bladder) may contribute to the observed increase in cell size (Vizzard 2000).

Bladder inflammation significantly increased the excitability of both TL and LS bladder neurons, consistent with a prior study that examined the properties of LS neurons in the same model (Yoshimura and de Groat 1999). Although not the focus of the present study, we and others have previously demonstrated that increased excitability during visceral inflammation is due to an increase in tetrodotoxin (TTX)-resistant sodium currents and a decrease in A-type potassium current (Bielefeldt et al. 2002; Dang et al. 2004; Stewart et al. 2003; Yoshimura and de Groat 1999). We also noted the appearance of spontaneous activity in both afferent pathways (i.e., LS and TL DRG neurons), similar to findings for the stomach after gastric inflammation (Dang et al. 2005b). This was associated with apparent membrane potential oscillations in cells from CYP-treated animals. Changes in the properties of voltage-sensitive sodium currents and/or potassium channels are thought to contribute to membrane potential oscillations and may play an important role in the pathogenesis of neuropathic pain (Amir et al. 1999, 2002; Kapoor et al. 1997). In support, we noted a significantly longer duration of the action potential in both LS and TL neurons from CYP-treated rats, suggesting changes in expression/properties of TTX-resistant and/or A-type potassium channels.

In contrast to control conditions, a greater proportion of TL bladder neurons responded to purinergic agonists after bladder inflammation. Considering the important role of ATP in the regulation of micturition, the present results may provide an explanation for the increased contribution of splanchnic bladder afferents in conveying sensory information during cystitis (Mitsui et al. 2001). In both TL and LS neurons, we observed an increase in peak current density in response to purinergic stimulation, consistent with a reported increase in the peripheral purinergic component in a model of colitis (Wynn et al. 2004). We could not quantify P2X proteins because only about 5–6% of LS DRG neurons are bladder neurons, but it is likely that the increase in peak current density is due to an increase in the expression of purinergic receptors. First, experiments were performed 3–10 h after removal and dissociation of DRG neurons. Therefore G-protein–mediated effects (e.g., changes in phosphorylation status of the channels) cannot explain differences in currents between cells obtained from controls and animals with cystitis because these effects would have reversed within this time frame. Second, we noted an increase in the proportion of TL neurons responding to purinergic agonists. Together with immunohistochemical evidence showing a significant increase in the proportion of TL neurons immunopositive for $P2X_3$, this suggests de novo synthesis of P2X receptors in neurons that do not normally express P2X receptors. Finally, the increase in peak current density was associated with an increase in the maximum current rather than a change in the EC_{50}. Consistent with this interpretation, others have demonstrated an increase in $P2X_3$ receptor protein after inflammation of the hind limb footpad (Xu and Huang 2002), presumably due to up-regulation of P2X receptor transcripts by NGF (Ramer et al. 2001), which is also increased after bladder inflammation (Lamb et al. 2004; Vizzard 2000). We did not directly

examine input resistance of bladder neurons following CYP treatment. However, Yoshimura and De Groat (1999) previously demonstrated an increase in input resistance associated with a reduction in A-type potassium current in bladder neurons following CYP treatment. They concluded that a reduction in A-type potassium current contributes to bladder neuron hyperexcitability following CYP treatment. The present report provides evidence that CYP treatment increases P2X currents, which contribute, in part, to the hyperexcitability of bladder neurons.

Current kinetics and pharmacologic data suggest that the slow desensitizing current (seen predominantly in LS neurons) is primarily due to activation of heteromeric $P2X_{2/3}$ receptors, while the fast desensitizing current (predominant in TL neurons) is mediated by homomeric $P2X_3$ receptors (for a more detailed discussion, see Dang et al. 2005a and Zhong et al. 2003). Both purinergic agonists triggered only a slow desensitizing current in LS neurons from CYP-treated rats, whereas ATP and *α*,*β*-metATP produced primarily mixed and fast desensitizing currents in TL counterparts, respectively, suggesting a differential regulation of P2X receptor expression after bladder inflammation. Because the maximum slow desensitizing current activated by ATP relative to *α*,*β*-metATP was reduced in bladder LS neurons after bladder inflammation, the present data suggest an increased expression of heteromeric $P2X_{2/3}$ receptors and further demonstrate the dominance of heteromeric $P2X_{2/3}$ receptors in LS neurons after bladder inflammation. In contrast, after inflammation, significantly more TL neurons expressed only a fast desensitizing current in response to *α*,*β*-metATP (compared with ATP), and the current was inhibited by both TNP-ATP and A317491. These results suggest that bladder inflammation up-regulates the expression of homomeric $P2X_3$ channels in TL neurons, consistent with an increase in the number of $P2X_3$-immunoreactive TL cells and a report by Wynn et al. (2004) that DRG neurons, which normally express CGRP but not $P2X_3$ receptors, also expressed $P2X_3$ receptors after colon inflammation. Furthermore, because *α*,*β*-metATP activated significantly fewer TL neurons that express mixed desensitizing currents after inflammation compared with control, the present findings suggest that heteromeric $P2X_{2/3}$ receptors are down-regulated in some TL neurons after bladder inflammation. Because heteromeric $P2X_{2/3}$ receptors desensitize significantly more slowly and recover faster than do homomeric receptors, we suggest that purinergic signals are predominantly transmitted through the pelvic rather the splanchnic pathway in the presence of ATP, especially in cystitis in which ATP release is increased substantially (Sun et al. 2001).

As already discussed in the context of changes in peak current density, G-protein–mediated changes in phosphorylation status are unlikely to account for the slower desensitization kinetics observed in LS neurons from CYP-treated rats. Rather, increases in the expression of other P2 receptors may slow desensitization kinetics for the slow desensitizing current. In support of this, increasing the proportion of $P2X_2$ relative to $P2X_3$ receptor expression progressively slows the desensitizing kinetics of the slow desensitizing current in a heterologous expression system (Liu et al. 2001).

In summary, bladder inflammation produces hyperexcitability and sensitizes bladder neurons in both the pelvic and splanchnic pathways. This hypersensitivity is associated with an increased expression and/or properties of homomeric $P2X_3$ and heteromeric $P2X_{2/3}$ receptors in TL and LS bladder neurons, respectively. The altered P2X receptor expression accounts for greater current density in response to purinergic agonists, and likely contributes to the slowed desensitization kinetics of the slow desensitizing current after bladder inflammation. Considering the reported mechanosensory role for homomeric $P2X_3$ and $P2X_2$ and heteromeric $P2X_{2/3}$ receptors (Cockayne et al. 2000, 2005; Rong et al. 2002; Vlaskovska et al. 2001), and the increased urothelial release of ATP during inflammation (Sun et al. 2001), the present findings suggest that the altered expression of P2X receptors contributes to the enhanced responses of bladder neurons during cystitis.

ACKNOWLEDGMENTS

We thank M. Jarvis (Abbott Laboratories) for the gift of A317491, M. Burcham for preparation of the graphics, and L. Burnes and S. Kardos for invaluable technical assistance.

GRANTS

This work was supported by National Institute of Neurological Disorders and Stroke Grant NS-35790.

REFERENCES

Amir R, Liu CN, Kocsis JD, Devor M. Oscillatory mechanism in primary sensory neurones. Brain 2002;125:421–435. [PubMed: 11844741]

Amir R, Michaelis M, Devor M. Membrane potential oscillations in dorsal root ganglion neurons: role in normal electrogenesis and neuropathic pain. J Neurosci 1999;19:8589–8596. [PubMed: 10493758]

Andersson KE. Bladder activation: afferent mechanisms. Urology 2002;59:43–50. [PubMed: 12007522]

Applebaum AE, Vance WH, Coggeshall RE. Segmental localization of sensory cells that innervate the bladder. J Comp Neurol 1980;192:203–209. [PubMed: 7400394]

Bielefeldt K, Ozaki N, Gebhart GF. Experimental ulcers alter voltage-sensitive sodium currents in rat gastric sensory neurons. Gastroenterology 2002;122:394–405. [PubMed: 11832454]

Brierley SM, Jones RCW 3rd, Gebhart GF, Blackshaw LA. Splanchnic and pelvic mechanosensory afferents signal different qualities of colonic stimuli in mice. Gastroenterology 2004;127:166–178. [PubMed: 15236183]

Bon K, Lanteri-Minet M, Menetrey D, Berkley KJ. Sex, time of day and estrous variations in behavioral and bladder histological consequences of cyclophospamide-induced cystitis in rats. Pain 1997;73:423–429. [PubMed: 9469534]

Bon K, Lichtensteiger CA, Wilson SG, Mogil JS. Characterization of cyclophosphamide cystitis, a model of visceral and referred pain, in the mouse: species and strain differences. J Urol 2003;170:1008–1012. [PubMed: 12913760]

Burkman RT. Chronic pelvic pain of bladder origin: epidemiology, pathogenesis and quality of life. J Reprod Med 2004;49:225–229. [PubMed: 15088860]

Cockayne DA, Dunn PM, Zhong Y, Rong W, Hamilton SG, Knight GE, Ruan HZ, Ma B, Yip P, Nunn P, McMahon SB, Burnstock G, Ford AP. P2X2 knockout mice and P2X2/P2X3 double knockout mice reveal a role for the P2X2 receptor subunit in mediating multiple sensory effects of ATP. J Physiol 2005;567:621–639. [PubMed: 15961431]

Cockayne DA, Hamilton SG, Zhu QM, Dunn PM, Zhong Y, Novakovic S, Malmberg AB, Cain G, Berson A, Kassotakis L, Hedley L, Lachnit WG, Burnstock G, McMahon SB, Ford AP. Urinary bladder hyporeflexia and reduced pain-related behaviour in P2X3-deficient mice. Nature 2000;407:1011–1015. [PubMed: 11069181]

Cox PJ. Cyclophosphamide cystitis—identification of acrolein as the causative agent. Biochem Pharmacol 1979;28:2045–2049. [PubMed: 475846]

Dang K, Bielefeldt K, Gebhart GF. Gastric ulcers reduce A-type potassium currents in rat gastric sensory ganglion neurons. Am J Physiol Gastrointest Liver Physiol 2004;286:G573–G579. [PubMed: 14525728]

Dang K, Bielefeldt K, Gebhart GF. Differential responses of bladder lumbosacral and thoracolumbar dorsal root ganglion neurons to purinergic agonists, protons, and capsaicin. J Neurosci 2005a; 25:3973–3984. [PubMed: 15829649]

Dang K, Bielefeldt K, Lamb K, Gebhart GF. Gastric ulcers evoke hyperexcitability and enhance P2X receptor function in rat gastric sensory neurons. J Neurophysiol 2005b;93:3112–3119. [PubMed: 15673552]

Dang K, Burnes L, Kardos S, Bielefeldt K, Gebhart GF. Cyclophosphamide-induced bladder inflammation enhances P2X receptor function and sensitizes rat lumbosacral and thoracolumbar dorsal root ganglion neurons. Soc Neurosci Abstr 2005c;170.2

Ferguson DR, Kennedy I, Burton TJ. ATP is released from rabbit urinary bladder epithelial cells by hydrostatic pressure changes—a possible sensory mechanism? J Physiol 1997;505:503–511. [PubMed: 9423189]

Ford APDW, Gever JR, Nunn PA, Zhong Y, Cefalu JS, Dillon MP, Cockayne DA. Purinoceptors as therapeutic targets for lower urinary tract dysfunction. Br J Pharmacol 2006;147:S132–S143. [PubMed: 16465177]

Gold MS, Traub RJ. Cutaneous and colonic rat DRG neurons differ with respect to both baseline and PGE2-induced changes in passive and active electrophysiological properties. J Neurophysiol 2004;91:2524–2531. [PubMed: 14736864]

Jarvis MF, Burgard EC, McGaraughty S, Honore P, Lynch K, Brennan TJ, Subieta A, Van Biesen T, Cartmell J, Bianchi B, Niforatos W, Kage K, Yu H, Mikusa J, Wismer CT, Zhu CZ, Chu K, Lee CH, Stewart AO, Polakowski J, Cox BF, Kowaluk E, Williams M, Sullivan J, Faltynek C. A-317491, a novel potent and selective non-nucleotide antagonist of P2X3 and P2X2/3 receptors, reduces chronic inflammatory and neuropathic pain in the rat. Proc Natl Acad Sci USA 2002;99:17179–17184. [PubMed: 12482951]

Kapoor R, Li YG, Smith KJ. Slow sodium-dependent potential oscillations contribute to ectopic firing in mammalian demyelinated axons. Brain 1997;120:647–652. [PubMed: 9153126]

Kirkemo A, Peabody M, Diokno AC, Afanasyev A, Nyberg LM Jr, Landis JR, Cook YL, Simon LJ. Associations among urodynamic findings and symptoms in women enrolled in the Interstitial Cystitis Data Base (ICDB) Study. Urology 1997;49:76–80. [PubMed: 9146005]

Kontani H, Hayashi K. Urinary bladder response to hypogastric nerve stimulation after bilateral resection of the pelvic nerve or spinal cord injury in rats. Int J Urol 1997;4:394–400. [PubMed: 9256330]

Lamb K, Gebhart GF, Bielefeldt K. Increased nerve growth factor expression triggers bladder overactivity. J Pain 2004;5:150–156. [PubMed: 15106127]

Lamb K, Kang YM, Gebhart GF, Bielefeldt K. Gastric inflammation triggers hypersensitivity to acid in awake rats. Gastroenterology 2003;125:1410–1418. [PubMed: 14598257]

Lanteri-Minet M, Bon K, de Pommery J, Michiels JF, Menetrey D. Cyclophosphamide cystitis as a model of visceral pain in rats: model elaboration and spinal structures involved as revealed by the expression of c-Fos and Krox-24 proteins. Exp Brain Res 1995;105:220–232. [PubMed: 7498375]

Liu M, King BF, Dunn PM, Rong W, Townsend-Nicholson A, Burnstock G. Coexpression of P2X(3) and P2X(2) receptor subunits in varying amounts generates heterogeneous populations of P2X receptors that evoke a spectrum of agonist responses comparable to that seen in sensory neurons. J Pharmacol Exp Ther 2001;296:1043–1050. [PubMed: 11181939]

Meen M, Coudore-Civiale MA, Eschalier A, Boucher M. Involvement of hypogastric and pelvic nerves for conveying cystitis induced nociception in conscious rats. J Urol 2001;166:318–322. [PubMed: 11435893]

Mitsui T, Kakizaki H, Matsuura S, Ameda K, Yoshioka M, Koyanagi T. Afferent fibers of the hypogastric nerves are involved in the facilitating effects of chemical bladder irritation in rats. J Neurophysiol 2001;86:2276–2284. [PubMed: 11698518]

Moss NG, Harrington WW, Tucker MS. Pressure, volume, and chemosensitivity in afferent innervation of urinary bladder in rats. Am J Physiol Regul Integr Comp Physiol 1997;272:R695–R703.

Ness TJ, Powell-Boone T, Cannon R, Lloyd LK, Fillingim RB. Psychophysical evidence of hypersensitivity in subjects with interstitial cystitis. J Urol 2005;173:1983–1987. [PubMed: 15879797]

Nicholas RS, Winter J, Wren P, Bergmann R, Woolf CJ. Peripheral inflammation increases the capsaicin sensitivity of dorsal root ganglion neurons in a nerve growth factor-dependent manner. Neuroscience 1999;91:1425–1433. [PubMed: 10391448]

Nickel JC. Interstitial cystitis: a chronic pelvic pain syndrome. Med Clin North Am 2004;88:467–481. [PubMed: 15049588]

North RA. Molecular physiology of P2X receptors. Physiol Rev 2002;82:1013–1067. [PubMed: 12270951]

Parsons CL. Interstitial cystitis: epidemiology and clinical presentation. Clin Obstet Gynecol 2002;45:242–249. [PubMed: 11862076]

Ramer MS, Bradbury EJ, McMahon SB. Nerve growth factor induces P2X(3) expression in sensory neurons. J Neurochem 2001;77:864–875. [PubMed: 11331415]

Rapp DE, Lyon MB, Bales GT, Cook SP. A role for the P2X receptor in urinary tract physiology and in the pathophysiology of urinary dysfunction. Eur Urol 2005;48:303–308. [PubMed: 15963632]

Rong W, Spyer KM, Burnstock G. Activation and sensitisation of low and high threshold afferent fibres mediated by P2X receptors in the mouse urinary bladder. J Physiol 2002;541:591–600. [PubMed: 12042363]

Stewart T, Beyak MJ, Vanner S. Ileitis modulates potassium and sodium currents in guinea pig dorsal root ganglia sensory neurons. J Physiol 2003;552:797–807. [PubMed: 12923214]

Sugiura T, Bielefeldt K, Gebhart GF. TRPV1 function in mouse colon sensory neurons is enhanced by metabotropic 5-hydroxytryptamine receptor activation. J Neurosci 2004;24:9521–9530. [PubMed: 15509739]

Sugiura T, Bielefeldt K, Gebhart GF. Mouse colon sensory neurons detect extracellular acidosis via TRPV1. Am J Physiol Cell Physiol 2007;292:C1768–C1774. [PubMed: 17251322]

Sun Y, Keay S, De Deyne PG, Chai TC. Augmented stretch activated adenosine triphosphate release from bladder uroepithelial cells in patients with interstitial cystitis. J Urol 2001;166:1951–1956. [PubMed: 11586266]

Tanaka K, Matsugami T, Chiba T. The origin of sensory innervation of the peritoneum in the rat. Anat Embryol 2002;205:307–313. [PubMed: 12136261]

Tempest HV, Dixon AK, Turner WH, Elneil S, Sellers LA, Ferguson DR. P2X and P2X receptor expression in human bladder urothelium and changes in interstitial cystitis. BJU Int 2004;93:1344–1348. [PubMed: 15180635]

Tubaro A. Defining overactive bladder: epidemiology and burden of disease. Urol 2004;64:2–6. [PubMed: 15621220]

Virginio C, Robertson G, Surprenant A, North RA. Trinitrophenyl-substituted nucleotides are potent antagonists selective for P2X1, P2X3, and heteromeric P2X2/3 receptors. Mol Pharmacol 1998;53:969–973. [PubMed: 9614197]

Vizzard MA. Changes in urinary bladder neurotrophic factor mRNA and NGF protein following urinary bladder dysfunction. Exp Neurol 2000;161:273–284. [PubMed: 10683293]

Vlaskovska M, Kasakov L, Rong W, Bodin P, Bardini M, Cockayne DA, Ford AP, Burnstock G. P2X3 knock-out mice reveal a major sensory role for urothelially released ATP. J Neurosci 2001;21:5670–5677. [PubMed: 11466438]

Wang HF, Shortland P, Park MJ, Grant G. Retrograde and transganglionic transport of horseradish peroxidase-conjugated cholera toxin B subunit, wheatgerm agglutinin and isolectin B4 from Griffonia simplicifolia I in primary afferent neurons innervating the rat urinary bladder. Neuroscience 1998;87:275–288. [PubMed: 9722157]

Wynn G, Ma B, Ruan HZ, Burnstock G. Purinergic component of mechanosensory transduction is increased in a rat model of colitis. Am J Physiol Gastrointest Liver Physiol 2004;287:G647–G657. [PubMed: 15331354]

Xu GY, Huang LY. Peripheral inflammation sensitizes P2X receptor-mediated responses in rat dorsal root ganglion neurons. J Neurosci 2002;22:93–102. [PubMed: 11756492]

Yoshimura N, de Groat WC. Increased excitability of afferent neurons innervating rat urinary bladder after chronic bladder inflammation. J Neurosci 1999;19:4644–4653. [PubMed: 10341262]

Yoshimura N, Seki S, Erickson KA, Erickson VL, Hancellor MB, de Groat WC. Histological and electrical properties of rat dorsal root ganglion neurons innervating the lower urinary tract. J Neurosci 2003;23:4355–4361. [PubMed: 12764124]

Zhong Y, Banning AS, Cockayne DA, Ford AP, Burnstock G, McMahon SB. Bladder and cutaneous sensory neurons of the rat express different functional P2X receptors. Neuroscience 2003;120:667–675. [PubMed: 12895508]

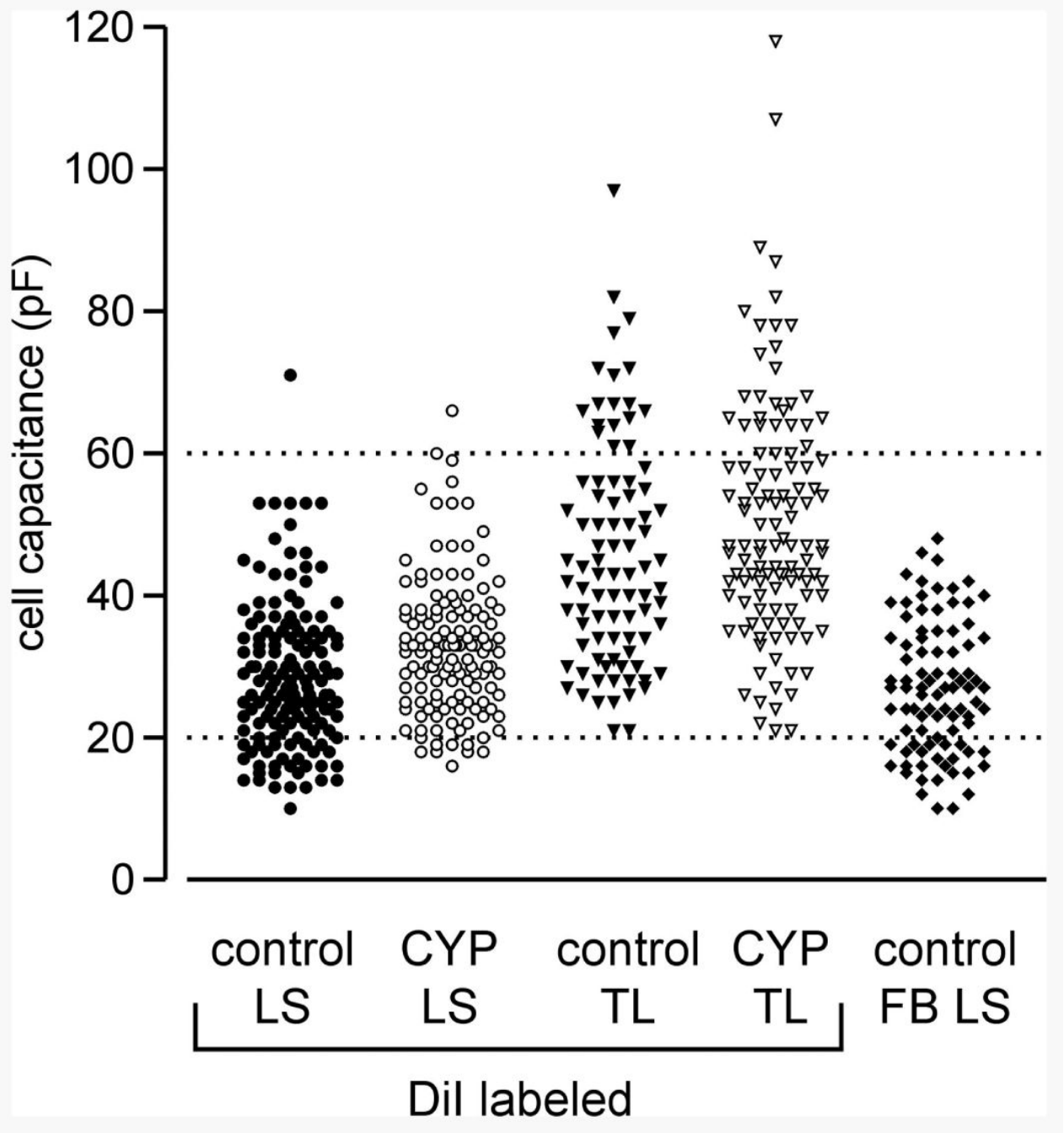

FIG. 1.

Distribution of whole cell capacitance in lumbosacral (LS) and thoracolumbar (TL) bladder sensory neurons from control and cyclophosphamide (CYP)-treated rats. No cells had a capacitance <20 pF in TL dorsal root ganglia (DRGs), whereas significantly fewer LS than TL neurons had a capacitance >60 pF. Bladder inflammation significantly increased the mean capacitance of both LS and TL neurons. Control LS bladder neurons labeled with fast blue (FB) showed a similar distribution of capacitance compared with DiI-labeled cells.

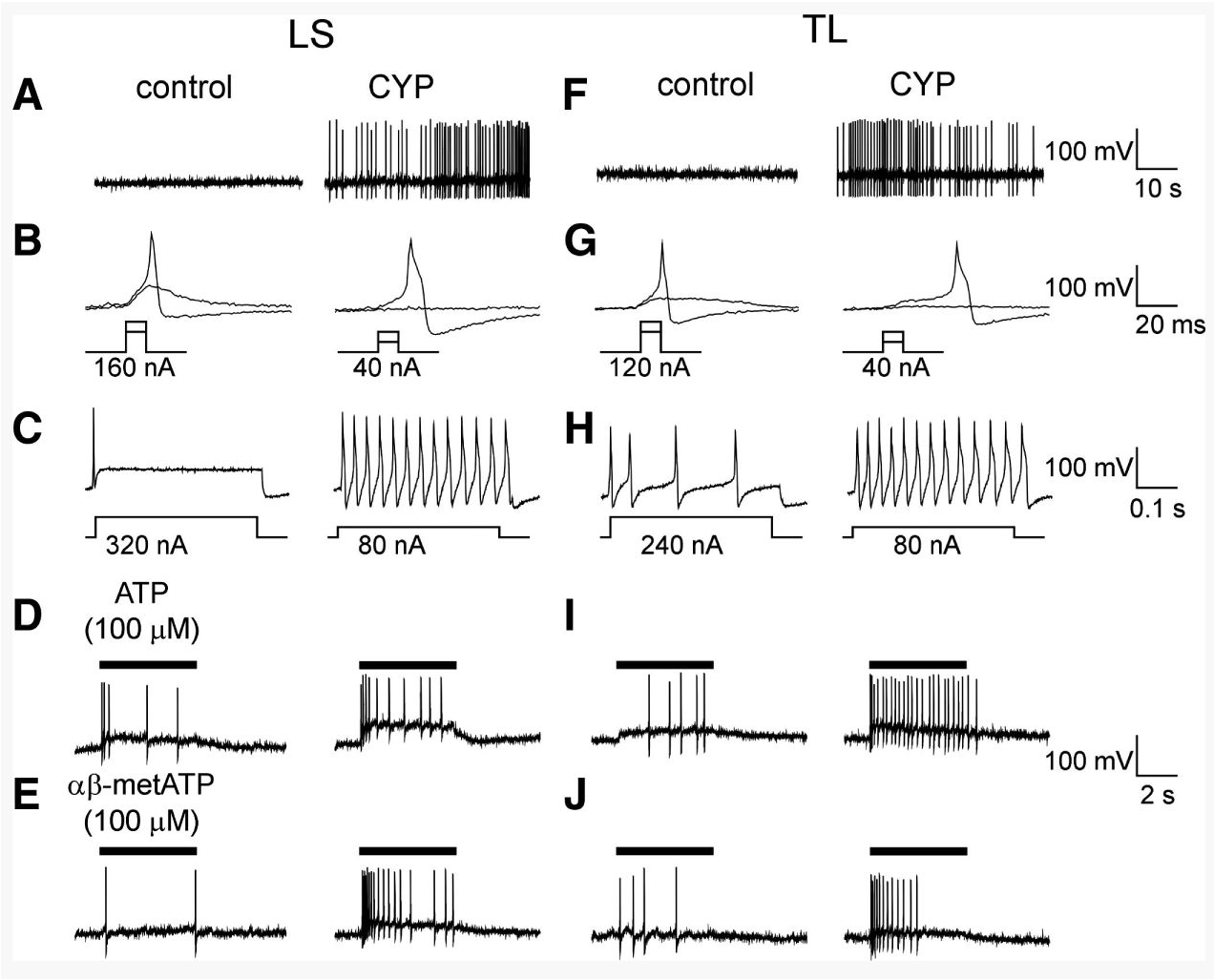

FIG. 2.

Passive and active properties of bladder neurons from control and CYP-treated rats examined in current-clamp mode. Examples illustrate that neither LS (*A*, *left trace*) nor TL (*F*, *left trace*) neurons were spontaneously active in the absence of bladder inflammation, but about one third of bladder neurons from CYP-treated rats exhibited spontaneous activity (*A* and *F*, *right traces*). Bladder inflammation reduced the rheobase current for action potential (AP) generation in both LS and TL bladder neurons (*B* and *G*, respectively) and increased the width of the AP. *C* and *H* show in the cells shown in *B* and *G* that current injection (500 ms) produced significantly more APs after bladder inflammation. Similarly, adenosine triphosphate (ATP, *D* and *I*) and *α*,*β*-metATP (*E* and *J*) depolarized LS and TL bladder neurons and produced greater depolarizations and more APs in cells from CYP-treated rats.

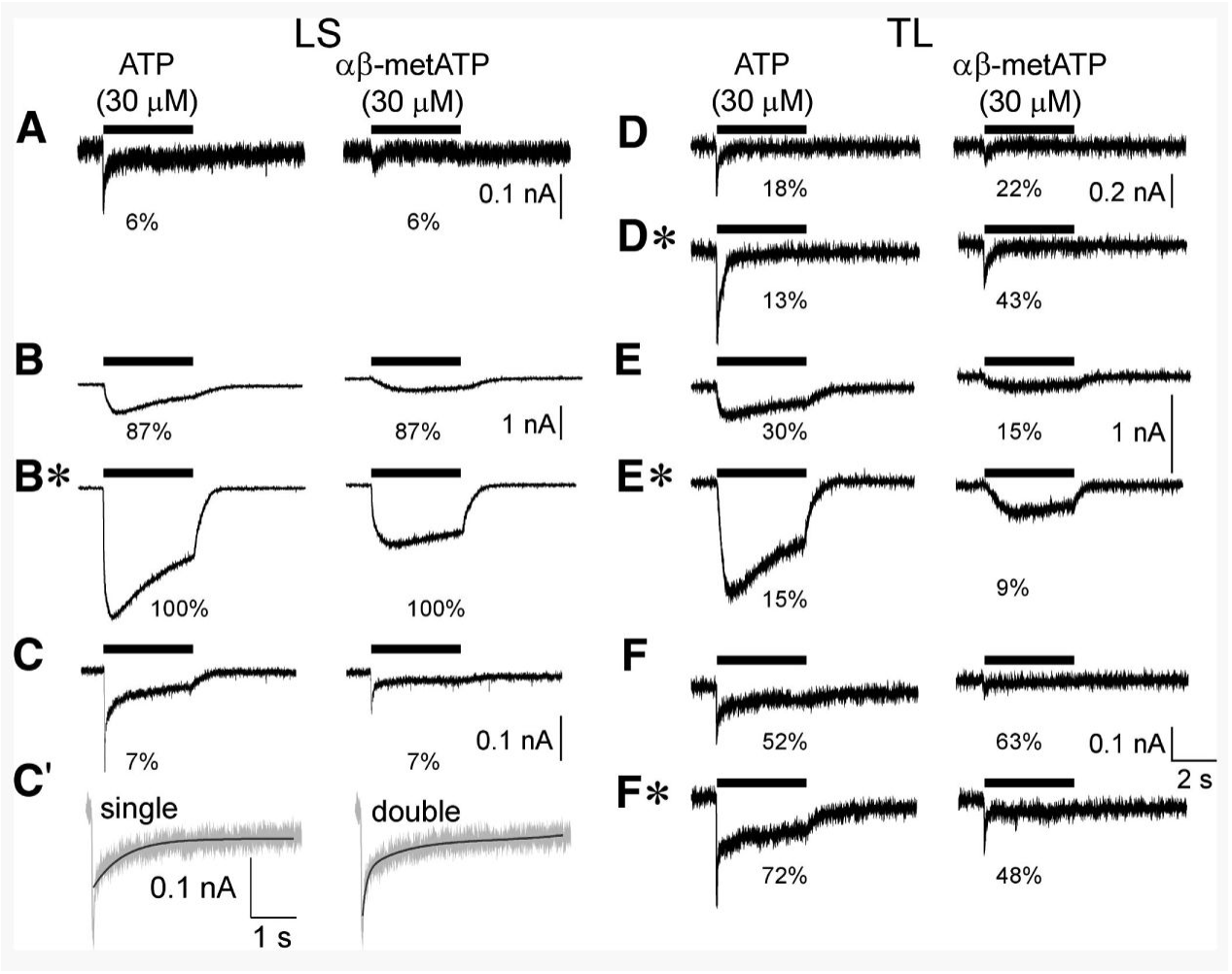

FIG. 3.

Purinergic agonist-activated inward currents in bladder sensory neurons were characterized based on desensitization kinetics as fast (*A* and *D*), slow (*B* and *E*), and mixed (*C* and *F*). To illustrate best exponential fits, we expanded the magnitude and timescale of records (e.g., *C*, *left trace*) and fitted with either a single or double exponential (*C′*). In neurons with mixed current kinetics, a double exponential always produced the best fit. In both LS and TL bladder neurons, the P2X receptor subtype-selective agonist *α*,*β*-metATP produced currents with kinetics similar to that triggered by ATP, but with significantly less current than did ATP in the same cells (corresponding *right traces* of each pair). In LS bladder neurons, the slow desensitizing current predominated (87% of 52 cells), whereas mixed currents were more common in TL neurons (52% of 27 cells). In cells from CYP-treated rats, both ATP and *α*,*β*-metATP produced greater magnitude, but only slow desensitizing currents in LS neurons (*B**). Bladder inflammation significantly increased the number of TL bladder neurons that responded to these purinergic agonists (see Table 2) and fast (*D**), slow (*E**), and mixed (*F**) desensitizing currents were all greater in magnitude relative to control.

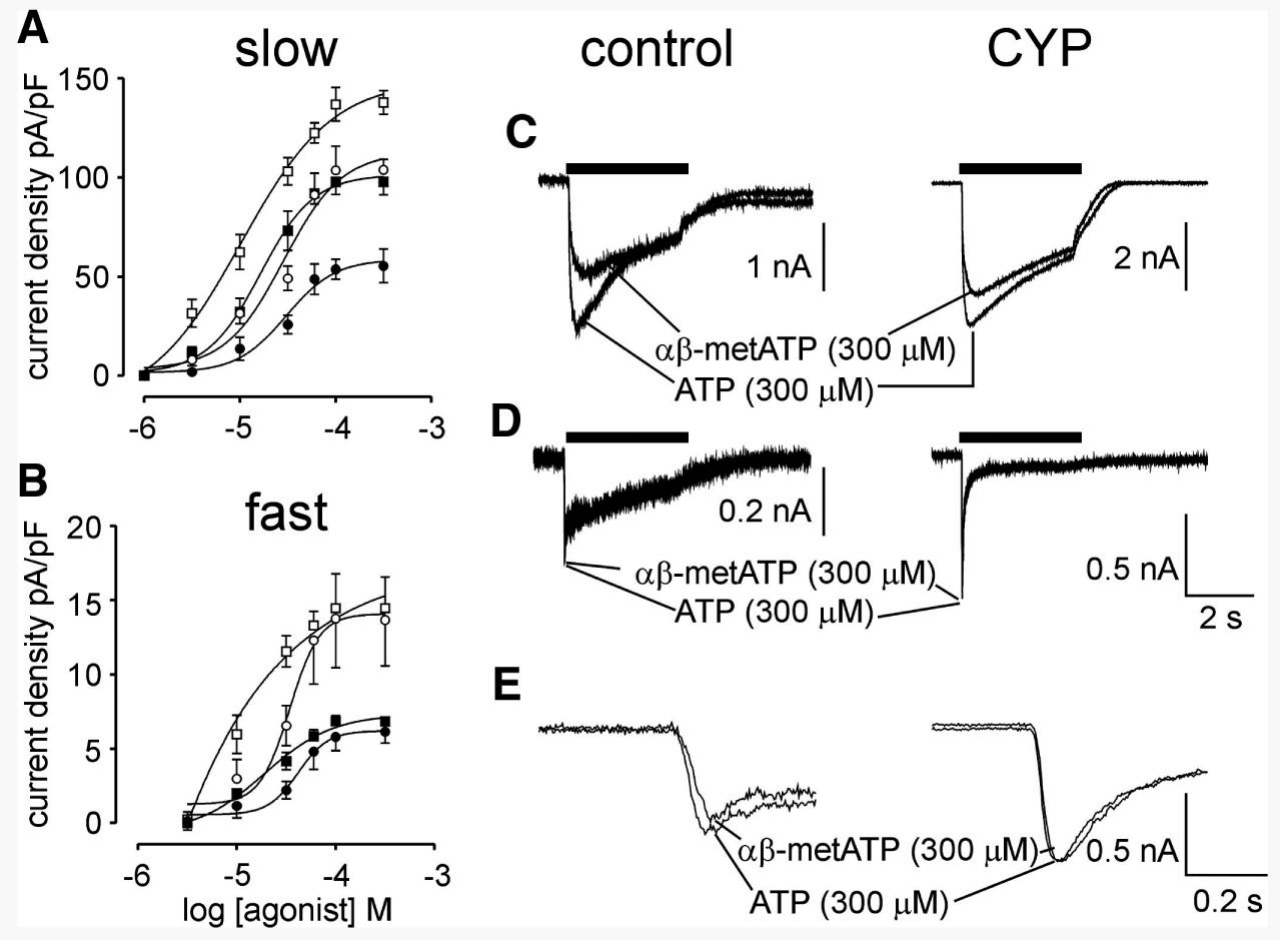

FIG. 4.

Dose–response relationship for control slow (*A*) and fast (*B*) desensitizing currents produced by ATP ■ and *α*,*β*-metATP (●), plotted as current density (pA/pF). ATP is significantly more potent than *α*,*β*-metATP for both kinetically distinct currents. Bladder inflammation did not alter the effective median concentration (EC_{50}) values for the slow □ or fast ○ desensitizing current (see text). When current densities were plotted against agonist concentrations using the same control cells, ATP ■ produced a significantly greater current density than *α*,*β*-metATP (●) for the slow (*A*) but not fast (*B*) desensitizing current. After bladder inflammation, ATP □ and *α*,*β*-metATP ○ produced significantly greater current densities for both the slow (*A*) and fast (*B*) desensitizing currents. To directly compare the fraction of slow and fast desensitizing current produced by *α*,*β*-metATP relative to ATP, we applied maximal concentrations of ATP (300 *μ*M) or *α*,*β*-metATP (300 *μ*M) to the same cells. ATP and *α*,*β*-metATP produced similar current amplitudes for the fast desensitizing current (examples in *D* and *E*, expanded timescale), but ATP produced 58 ± 3.8% (*n* = 11) more current than did *α*,*β*-metATP for the slow desensitizing current (*C, left traces*). In cells from CYP-treated rats, the magnitude of the slow desensitizing current produced by ATP and *α*,*β*-metATP was increased and ATP produced significantly less current difference (24.1 ± 2%; *n* = 9; *C, right traces*).

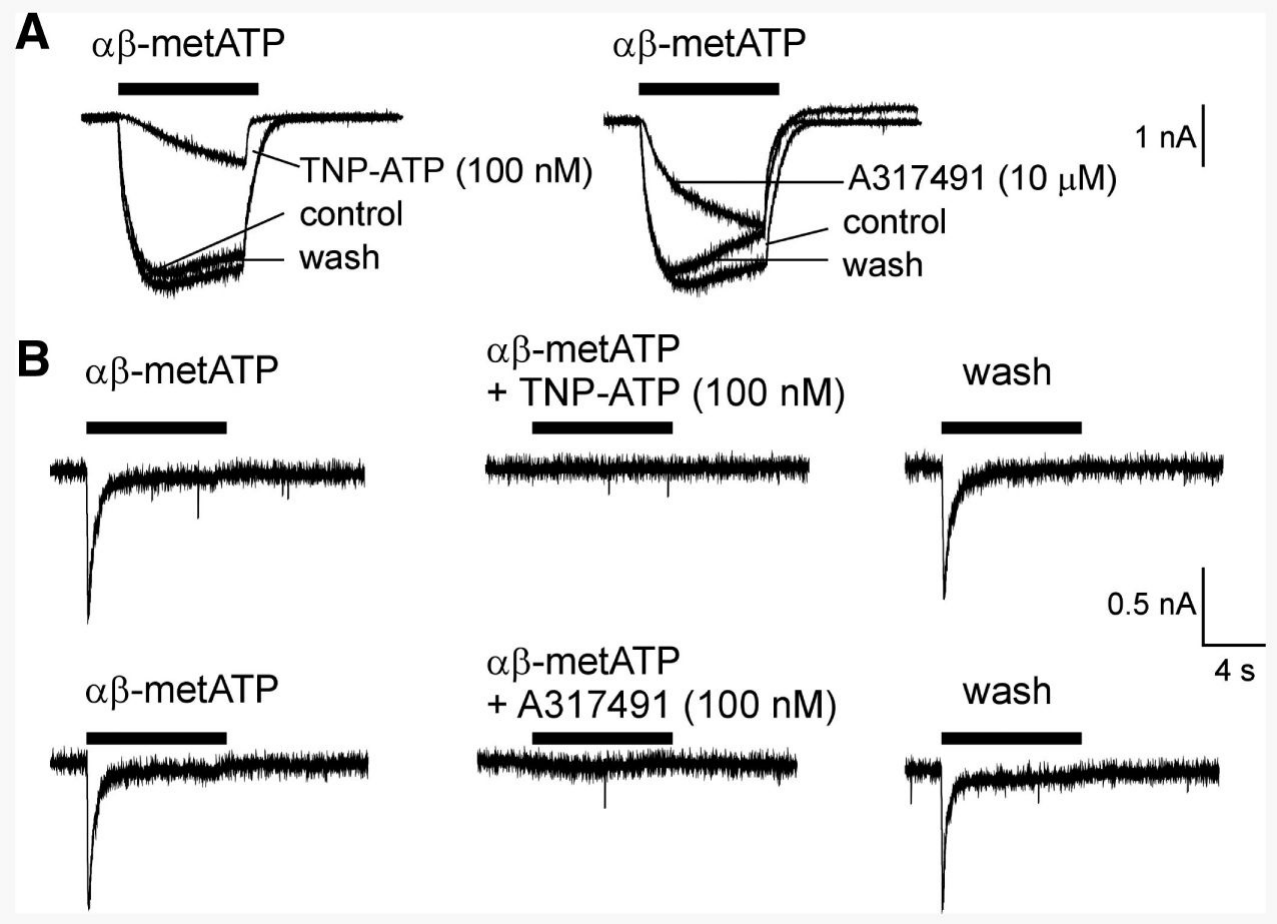

FIG. 5.

Antagonism of *α,β*-metATP-produced currents in neurons from CYP-treated rats. Examples illustrate about 75% antagonism of the slow current by TNP-ATP (100 nM) (*A*, *left traces*), but partial antagonism by A317491 (10 μM) (*A*, *right traces*) in the same cell. Both antagonists abolished the fast desensitizing current in the same cell (*B*) at a concentration of 100 nM, which for A317491 is a significantly lower concentration than the incomplete antagonism of the slow desensitizing current (*A*, *right*). *α,β*-metATP-produced currents recovered completely after washout of antagonists.

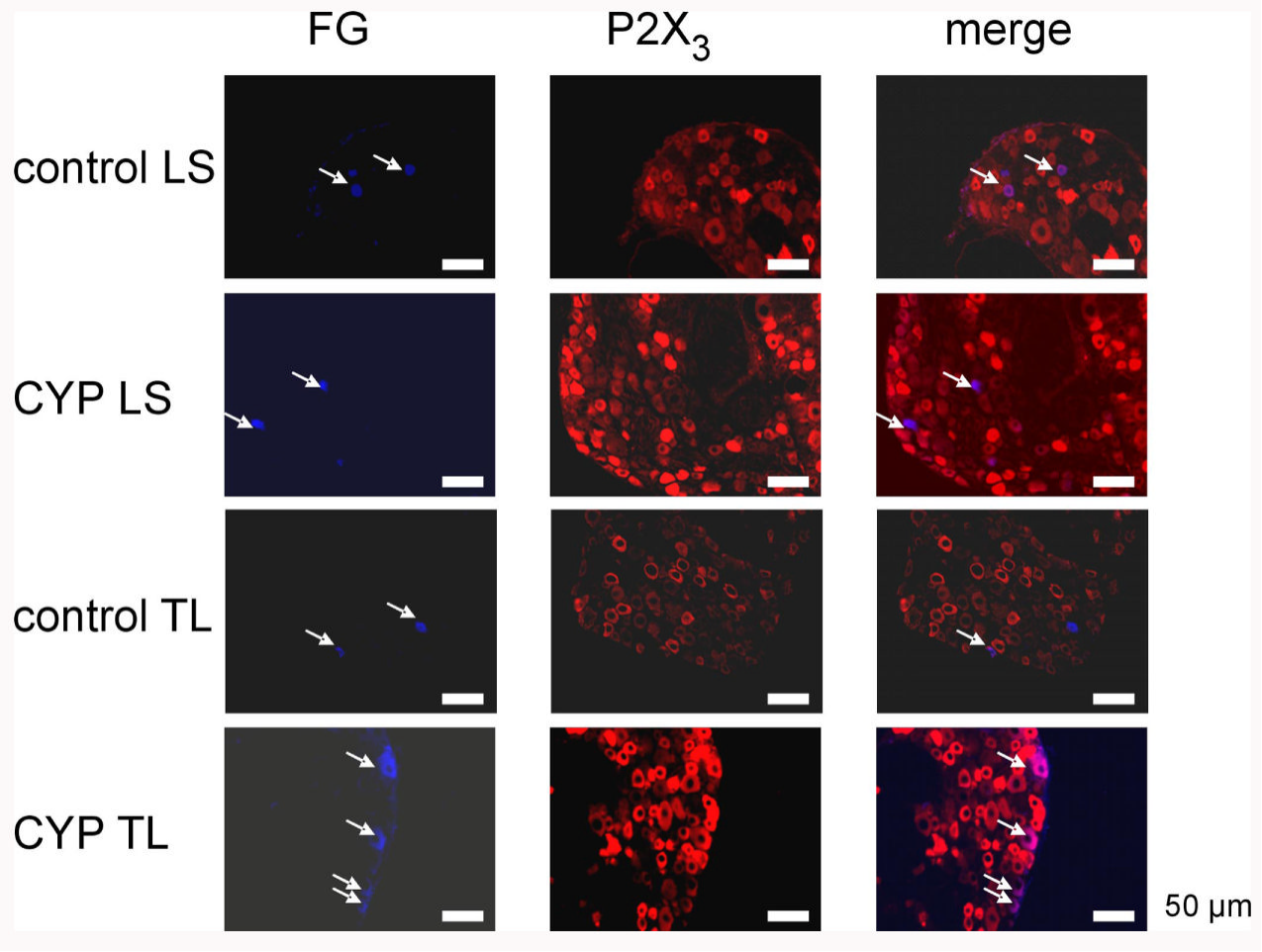

FIG. 6.

Immunohistochemistry of bladder neurons from CYP-treated and control rats. Fluorogold (FG; *left column*) was used to retrogradely label LS and TL bladder neurons (arrows), which were counterstained with $P2X_3$ antibody (*middle column*). Merging the *left* and *middle columns* confirmed that bladder sensory neurons were immunoreactive for $P2X_3$ (*right column*; arrows indicate colocalization).

TABLE 1

Passive and active electrical properties of LS and TL bladder neurons from CYP-treated and control rats

Property	Treatment	LS	TL
	A. Current injection		
RMP, mV	Control	−55.02 ± 2.1	−47.78 ± 1.0*
	CYP	−55.34 ± 1.6	−49.61 ± 1.3
Spontaneous activity	Control	0/23 (0%)	0/23 (0%)
	CYP	11/31 (35%)†	13/29 (45%)†
Rheobase, pA	Control	146.1 ± 14.5	95.7 ± 7.5*
	CYP	66.2 ± 6.2†	50.6 ± 5.5†
Rheobase, pA/pF	Control	5.67 ± 0.7	2.54 ± 0.2*
	CYP	2.28 ± 0.3†	1.14 ± 0.2†
AP threshold, mV	Control	−24.5 ± 1.4	−23.3 ± 0.7
	CYP	−30.1 ± 0.8†	−28.2 ± 1.0†
AP amplitude, mV	Control	87.9 ± 4.1	87.4 ± 2.1
	CYP	93.4 ± 2.2	89.9 ± 3.0
AP duration, ms	Control	3.1 ± 0.2	3.2 ± 0.2
	CYP	4.2 ± 0.3†	5.0 ± 0.6†
Rheobase × 2 (APs)	Control	5.0 ± 0.9	6.3 ± 0.6
	CYP	10.7 ± 2.1†	9.2 ± 0.7†
	B. ATP (100 μM)		
Depolarization, mV	Control	24.5 ± 1.5	6.2 ± 1.2*
	CYP	31.9 ± 1.5†	14.1 ± 1.2†
Number of APs	Control	8.9 ± 0.7	3.7 ± 1.4*
	CYP	15.2 ± 2.1†	13.5 ± 3.6†
	C. αβ-metATP (100 μM)		
Depolarization, mV	Control	15.3 ± 1.4	5.4 ± 1.1*
	CYP	25.6 ± 1.3†	13.2 ± 1.2†
Number of APs	Control	5.2 ± 0.7	2.4 ± 1.3*
	CYP	12.9 ± 0.9†	10.3 ± 1.4†

Values are means ± SE, or percentages.

*$P < 0.05$ versus LS counterparts

†$P < 0.05$ versus control (saline) treatment.

TABLE 2

Purinergic agonist-produced current densities for LS and TL bladder sensory neurons from CYP-treated and control rats

Property	Treatment	LS Neurons	TL Neurons
	A. ATP		
Percentage responding	Control	96% (53/55)	62% (33/53)*
	CYP	97% (59/61)	85% (47/55)†
Current density, pA/pF			
Fast current	Control	5.3 ± 0.6	4.4 ± 0.8
	CYP	n/a	9.9 ± 1.2†
Slow current	Control	67.8 ± 11.0	4.7 ± 0.7*
	CYP	116.2 ± 12.0†	8.7 ± 1.0†
Mixed current	Control	6.4 ± 0.4	5.6 ± 0.9
	CYP	n/a	10.4 ± 0.8†
	B. αβ-metATP		
Percentage responding	Control	95% (52/55)	51% (27/53)*
	CYP	92% (56/61)	80% (44/55)†
Current density, pA/pF			
Fast current	Control	2.1 ± 0.5	1.5 ± 0.3
	CYP	n/a	4.4 ± 0.4†
Slow current	Control	28.4 ± 4.0	2.4 ± 0.7*
	CYP	51.5 ± 5.0†	6.8 ± 0.2†
Mixed current	Control	2.7 ± 0.6	1.9 ± 0.3
	CYP	n/a	5.1 ± 0.7†

Values are means ± SE, or percentages.

n/a, not applicable.

* $P < 0.05$ between LS and TL neuron groups

† $P < 0.05$ between control and CYP treatment.

TABLE 3

Current kinetics for LS and TL bladder sensory neurons from CYP-treated and control rats

Current	Treatment	ATP (30 μM)			$\alpha\beta$-metATP (30 μM)		
		10–90% Rise Time, ms	Tau 1, ms	Tau 2, ms	10–90% Rise Time, ms	Tau 1, ms	Tau 1, ms
				A. LS			
Fast	Control	22.9 ± 4	4,475 ± 402	n/a	630.8 ± 47	12,990 ± 2,011	n/a
	CYP	n/a	n/a	n/a	n/a	n/a	n/a
Slow	Control	226.7 ± 38	4,475 ± 402	n/a	630.8 ± 47	3,723 ± 535	n/a
	CYP	125.2 ± 21*	6,820 ± 710*	n/a	404.0 ± 37*	12,990 ± 2,011*	n/a
Mixed	Control	26.7 ± 3	194 ± 58	3,419 ± 827	28.3 ± 3	218 ± 40	n/a
	CYP	n/a	n/a	n/a	n/a	n/a	n/a
				B. TL			
Fast	Control	22.7 ± 2	217 ± 42	n/a	25.9 ± 3	215 ± 29	n/a
	CYP	19.6 ± 3	196 ± 39	n/a	23.3 ± 2	223 ± 30	n/a
Slow	Control	258.0 ± 48	3,933 ± 827	n/a	269.8 ± 34	4,179 ± 1,075	n/a
	CYP	212.0 ± 19	2,953 ± 876	n/a	232.4 ± 18	3,287 ± 724	n/a
Mixed	Control	27.6 ± 3	239 ± 33	2,931 ± 252	22.1 ± 4	247 ± 37	3,857 ± 856
	CYP	24.3 ± 2	199 ± 21	3,473 ± 594	25.8 ± 3	212 ± 28	2,768 ± 594

Values are means ± SE.

n/a, not applicable.

*$P < 0.05$ versus the corresponding control group.